ELSEVIER

Physica B 307 (2001) 57–63

PHYSICA B

www.elsevier.com/locate/physb

Thermal conductivity anomalies around antiferromagnetic order in $La_{0.50}Sr_{0.50}MnO_3$ and $Nd_{0.50}Sr_{0.50}MnO_3$ crystals

Hiroyuki Fujishiro*

Faculty of Engineering, Iwate University, 4-3-5 Ueda, Morioka 020-8551, Japan

Received 5 March 2001; received in revised form 17 May 2001; accepted 11 June 2001

Abstract

The thermal conductivity $\kappa(T)$ has been measured for sintered-$La_{0.50}Sr_{0.50}MnO_3$ (S-LSMO) and $Nd_{0.50}Sr_{0.50}MnO_3$ fabricated by the floating zone method (FZ-NSMO) in magnetic fields up to 5 T. Both crystals commonly show a first order transition from the ferromagnetic (FM) to the antiferromagnetic (AF) phase with decreasing temperature and $\kappa(T)$ shows seemingly similar reductions just below the Néel temperature T_N in zero magnetic field. The field dependence of $\kappa(T)$ is, in contrast, quite different. $\kappa(T)$ of FZ-NSMO increases over the entire temperature range below T_N in applied fields because of the electronic-component (κ_e) enhancement. For S-LSMO, where the heat conduction is mainly due to phonons, $\kappa(T)$ hardly depends on the magnetic field except for the change corresponding to the T_N shift. Analyses suggest that the phonon scattering by conduction electrons is very strong in the metallic FM phase of FZ-NSMO.

PACS: 65.40.−b; 75.30.Kz; 72.15.Eeb; 66.30.Xj

Keywords: Thermal conductivity; $Nd_{0.50}Sr_{0.50}MnO_3$; $La_{0.50}Sr_{0.50}MnO_3$; Antiferromagnetic order; Magnetic structure; Phonon scattering

1. Introduction

A series of distorted perovskite manganese oxides of the formula, $RE_{1-X}AE_XMnO_3$ (RE: lanthanide earth ions, AE: alkaline earth ions), exhibit a variety of dramatic physical properties as a result of various competing interactions such as double exchange, antiferromagnetic (AF) superexchange, charge order (CO), orbital order (OO) and Jahn–Teller effect [1–3]. A typical manganese oxide such as $La_{1-X}Ca_XMnO_3$ shows a phase transition from a paramagnetic insulating (PM-I) state to a ferromagnetic metallic (FM-M) state upon cooling for $0.20 < X < 0.45$ and exhibits colossal magnetoresistance [4,5]. For further carrier doping at around $X = 0.5$ with $Mn^{3+}/Mn^{4+} \sim 1:1$, the FM-M state becomes unstable against the AF state, which has been intensively studied for $Nd_{0.50}Sr_{0.50}MnO_3$ [6,7], $Pr_{0.50}Sr_{0.50}MnO_3$ [6], $La_{0.50}Sr_{0.50}MnO_3$ [8] and so on. Among these systems, the $Nd_{1-X}Sr_XMnO_3$

*Corresponding author. Tel.: +81-19-621-6363; fax: +81-19-621-6373.

E-mail address: fujisiro@iwate-u.ac.jp (H. Fujishiro).

0921-4526/01/$ -see front matter
PII: S0921-4526(01)00624-X

(NSMO) system is a typical one well investigated at around $X = 0.5$, where the magnetic, structural and electronic structures are rather complicated [6,9]. The $X = 0.50$ sample of NSMO shows a FM-M state below $T_c \approx 270$ K and transforms to an AF insulating state below $T_N \approx 150$ K with the CE-type magnetic structure with CO. Recently, the complicated phase segregation between A-type AF, CE-type AF and FM phases was observed by neutron diffraction [10]. In contrast, the magnetic structure of $La_{1-X}Sr_XMnO_3$ (LSMO) around $X \sim 0.5$ is the A-type AF order without CO, which was confirmed for the $La_{0.46}Sr_{0.54}MnO_3$ single crystal [11,12] and the $La_{0.50}Sr_{0.50}MnO_3$ polycrystal [13].

Several theoretical and experimental studies have pointed out that the electron–phonon coupling and the local lattice distortion of MnO_6 octahedra play important roles in the anomalous transport properties of doped manganites [14,15]. The thermal conductivity κ is one of the valuable tools to investigate the lattice dynamics near phase transitions [16–19] as well as in neutron and electron diffraction studies. For the $X = 0.50$ manganite samples, the thermal conductivity $\kappa(T)$ seems to behave quite differently at low temperatures for various AF spin structures. $\kappa(T)$ of the $Pr_{0.50}Sr_{0.50}MnO_3$ crystal with the A-type spin structure drastically suppressed below T_N from the FM to AF state [16,18]. However, $\kappa(T)$ of $Pr_{0.50}Ca_{0.50}MnO_3$ and $La_{0.50}Ca_{0.50}MnO_3$ with the CE-type AF order shows a small anomaly at the CO transition temperature T_{CO} and/or at T_N from the paramagnetic (PM) state [18,19]. The relations between the $\kappa(T)$ anomaly around T_N and the magnetic structure and/or the existence of CO have not been thoroughly investigated. The application of a magnetic field to the manganese oxides systematically alters the electrical resistivity ρ, T_c and T_N. Therefore, the field dependence of the $\kappa(T)$ is expected to provide useful information about the origin of the $\kappa(T)$ anomaly around T_N. We report the temperature dependence of the thermal conductivity $\kappa(T)$ for $La_{0.50}Sr_{0.50}MnO_3$ and $Nd_{0.50}Sr_{0.50}MnO_3$ samples in applied fields up to 5 T and discuss the origin of the $\kappa(T)$ anomalies below T_N for both systems.

2. Experimental

The sintered-$La_{0.50}Sr_{0.50}MnO_3$ polycrystal (S-LSMO) was prepared by a standard solid-state reaction method. The preparation procedure was described in detail elsewhere [8]. The size of the S-LSMO sample is $3.2 \times 2.5 \times 12.0\,mm^3$ of which the measured density is 87% of the ideal one. The grain sizes observed by a scanning electron microscope were distributed between 20 and 40 μm. The $Nd_{0.50}Sr_{0.50}MnO_3$ crystal was prepared by a floating zone (FZ) method (FZ-NSMO). The raw powders of Nd_2O_3, $SrCO_3$ and Mn_3O_4 were calcined twice at 1000°C for 24 h in air and then pressed to a bar shape of ~ 6 mm ∅ in diameter and sintered twice at 1500°C for 8 h in air. A lamp image FZ furnace with quadruple ellipsoidal millers was utilized for the crystal growth. The crystal growth was performed at 8 mm/h in flowing air. The crystal was grown nearly parallel to the c-axis of the orthorhombic structure as was determined by X-ray diffraction analysis. The obtained crystal was heat-treated at 1700°C for 24 h in flowing O_2 gas to remove the thermal stress during the growth and to ensure the oxygen stoichiometry. The dimension of the FZ-NSMO crystal is $2.5 \times 2.5 \times 6.0\,mm^3$ in which the length of 6 mm is along the growth direction. The rectangular sample includes several single crystal grains with a size as large as ~ 1 mm.

The thermal conductivity $\kappa(T)$ was measured by a steady-state heat-flow method between 5 and 300 K using an automated measuring apparatus with double radiation shields [20]. The magnetic field was applied parallel to the heat flow. The chromel–constantan thermocouples with 76 μm ∅ in diameter were used as thermometers, which had been calibrated in the magnetic field. The electrical resistivity $\rho(T)$ was measured by a standard four-terminal method. For $\kappa(T)$ and $\rho(T)$ measurements, a Gifford McMahon cycle helium refrigerator was used as a cryostat. The magnetic field up to 5 T was applied for the $\kappa(T)$ and $\rho(T)$ measurements, using a cryocooler-cooled superconducting magnet. The magnetization $M(T)$ was measured by use of a superconducting quantum interference device (SQUID) magnetometer in magnetic fields up to 5 T in zero field cooling (ZFC) and field cooling (FC) scans.

3. Experimental results

3.1. Sintered-$La_{0.50}Sr_{0.50}MnO_3$ (S-LSMO) crystal

Figs. 1 and 2 show the temperature dependence of the magnetization $M(T)$ and the electrical resistivity $\rho(T)$ of the S-LSMO crystal in a magnetic field. As can be seen from the $M(T)$ curve in a field of 0.5 T [19], this specimen shows a FM transition at $T_c = 290$ K and transforms to AF order below $T_N = 160$ K upon cooling. The phase transition to the AF order shows hysteretic behavior. The FM transition temperature T_c increases and the AF transition temperature T_N decreases with increasing applied field. It should be noticed that the residual weak-FM moment exists below T_N in higher magnetic fields. In Fig. 2, the zero-field resistivity $\rho(T)$ is slightly inflected at $T_c = 290$ K and then increases moderately with decreasing temperature. Below $T_N \approx 160$ K, $\rho(T)$ somewhat sharply increases with hysteresis and then further increases with decreasing temperature. However, the $\rho(T)$ increase in the vicinity of T_N is only by a factor of about 2 and rather small, which may be characteristic for the A-type AF order without CO. The $\rho(T)$ value decreases with increasing magnetic field, but the metallic $\rho(T)$ behavior cannot be confirmed below T_N. Metallic

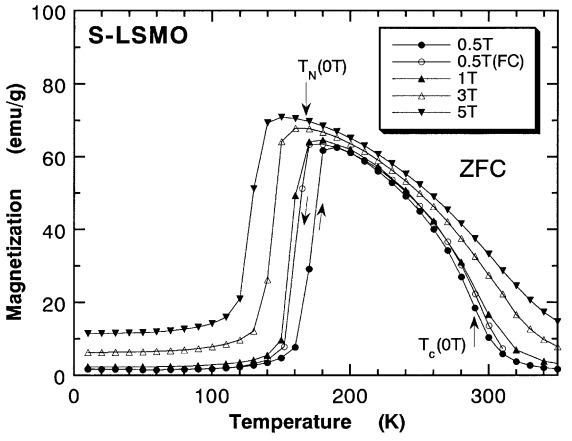

Fig. 1. Temperature dependence of the magnetization $M(T)$ of the sintered-$La_{0.50}Sr_{0.50}MnO_3$ (S-LSMO) crystal in magnetic fields after ZFC. The $M(T)$ data for the FC in $\mu_0 H = 0.5$ T are also presented.

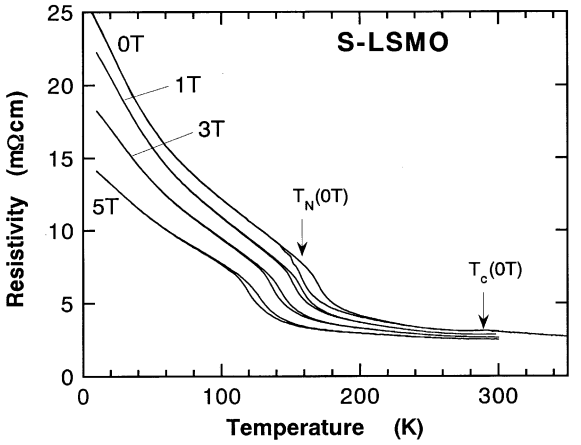

Fig. 2. Temperature dependence of the electrical resistivity $\rho(T)$ of the S-LSMO crystal in applied fields.

behavior of $\rho(T)$ was reported for a FZ-LSMO ($X = 0.54$) single crystal with A-type AF order by Akimoto et al. [11] The A-type LSMO ($X = 0.50$) thin film was fabricated by the pulsed laser deposition (PLD) method on a $SrTiO_3$ substrate, where the ratio of the lattice constants (c/a) could be set to be ≈ 1 and the AF and metallic $\rho(T)$ behavior was observed below T_N [21]. The in-plane resistivity of the $Nd_{0.45}Sr_{0.55}MnO_3$ single crystal with the A-type AF structure is metallic below T_N and the out-of-plane resisitivity is semiconductive [22]. The semiconductive $\rho(T)$ behavior of the present S-LSMO crystal shown in Fig. 2 may result from the effect of the c-axis oriented grains or some localization effect. Since sintered polycrystals are easy to realize a precise control of the hole content X and a uniform hole distribution, the AF transition from the FM order usually becomes sharper than that of the FZ-LSMO crystal.

Fig. 3 shows the temperature dependence of the thermal conductivity $\kappa(T)$ of the S-LSMO crystal in magnetic field. The $\kappa(T)$ curves in the FC runs are presented. In zero field, an anomalous reduction of $\kappa(T)$ is observed just below $T_N = 160$ K and then $\kappa(T)$ decreases with decreasing temperature. Below T_N, the application of the magnetic fields hardly affects $\kappa(T)$ except for the shift of the $\kappa(T)$ reduction point corresponding to the decrease of T_N. For $T > 160$ K, $\kappa(T)$ very slightly increases with increasing magnetic field.

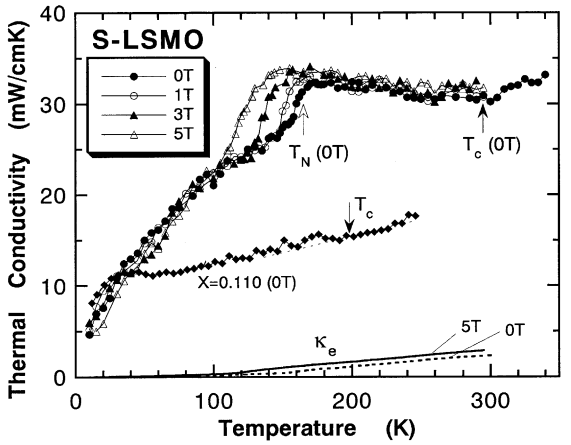

Fig. 3. Temperature dependence of the thermal conductivity $\kappa(T)$ of the S-LSMO crystal in applied fields after the FC. The electronic thermal conductivity $\kappa_e(T)$ at 0 and 5 T is also shown. For comparison, $\kappa(T)$ data of the sintered $La_{0.890}Sr_{0.110}MnO_3$ crystal in 0 T is included, in which the FM insulating state is stable over the entire range below T_c.

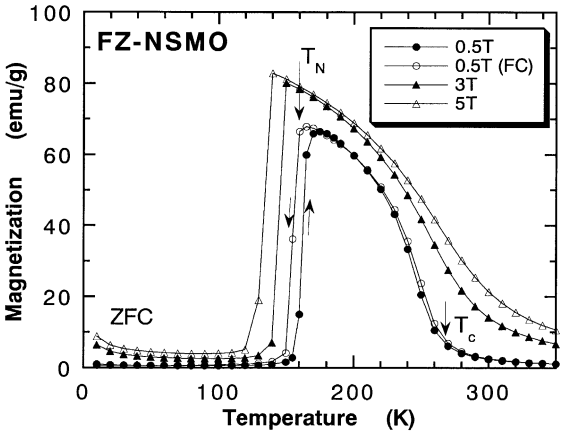

Fig. 4. Temperature dependence of the magnetization $M(T)$ of the FZ-$Nd_{0.50}Sr_{0.50}MnO_3$ (FZ-NSMO) crystal in applied fields after ZFC. The $M(T)$ data for the FC run for $\mu_0 H = 0.5$ T are also presented.

3.2. *FZ-$Nd_{0.50}Sr_{0.50}MnO_3$ (FZ-NSMO) crystal*

Figs. 4 and 5 show $M(T)$ and $\rho(T)$ of the FZ-NSMO crystal in magnetic field. The crystal shows an FM transition at $T_c = 265$ K and an AF transition at $T_N = 160$ K. When the higher magnetic field is applied to the sample, T_c increases and T_N decreases gradually, which is the behavior similar to that of the S-LSMO crystal shown in Fig. 1. In Fig. 5, $\rho(T)$ in the zero field decreases below $T_c = 265$ K and abruptly increases below $T_N = 150$ K about two orders of magnitude with large hysteresis. It is to be noticed that the temperature dependence of $\rho(T)$ of the present FZ-NSMO crystal are almost equal to that of the FZ-$Nd_{0.51}Sr_{0.49}MnO_3$ crystal reported by Kajimoto et al. [9]; the common features are the metallic $\rho(T)$ behavior below T_N and the relatively low $\rho(T)$ value at low temperatures ($\sim 10^1$ mΩ cm), which make a sharp contrast with the very large semiconductive $\rho(T)$ of the FZ-$Nd_{0.50}Sr_{0.50}MnO_3$ single crystal [6]. In the present FZ-NSMO crystal, the large enhancement of $\rho(T)$ at T_N makes a marked contrast with the small enhancement in S-LSMO and likely to correspond to the occurrence of CO in FZ-NSMO. However, it is also to be

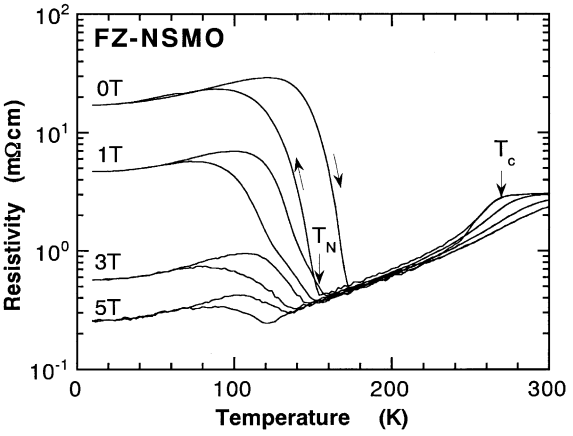

Fig. 5. Temperature dependence of the electrical resistivity $\rho(T)$ of the FZ-NSMO crystal in applied fields.

noticed that $\rho(T)$ of FZ-NSMO is rather metallic at low temperatures and this metallic $\rho(T)$ below T_N might suggest the coexistence of very small FM phase region with CE-type AF phase. The absolute value of $\rho(T)$ below T_N decreases with increasing applied field and $\rho(T)$ at 5 T is about two orders of magnitude smaller than that in 0 T.

Fig. 6 shows the temperature dependence of the thermal conductivity $\kappa(T)$ of FZ-NSMO under the magnetic fields in the FC runs. At zero field, $\kappa(T)$ shows a shallow dip around $T_c = 265$ K and an

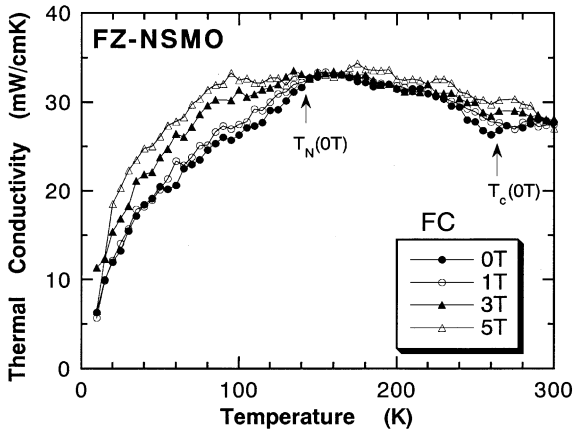

Fig. 6. Temperature dependence of the thermal conductivity $\kappa(T)$ of the FZ-NSMO crystal in applied fields in the FC runs.

anomalous reduction just below $T_N = 150\,K$ [23]. Below T_N, $\kappa(T)$ gradually increases with increasing magnetic field and above T_N $\kappa(T)$ also increases slightly. Hysteretic behavior of $\kappa(T)$ below T_N was also observed at $\mu_0 H = 0$ and 1 T which, however, was not confirmed at $\mu_0 H \geqslant 3\,T$ (not shown in the figure).

4. Discussion

The heat conduction in magnetic materials can be represented as the sum of phonon (κ_{ph}), electron (κ_e) and magnon (κ_m) contributions. In Fig. 3, we present $\kappa(T)$ of S-LSMO($X = 0.11$) which is a FM insulator. $\kappa(T)$ of this sample, which is very small over the entire temperature regime, shows almost no anomaly or enhancement below T_c. A close examination of the data suggests that the $\kappa(T)$ enhancement due to κ_m is about $\sim 1\,mW/cm\,K$ in the LSMO compound if it exists. Because there seems to be no special reason that κ_m is enhanced in S-LSMO($X = 0.50$) and in FZ-NSMO($X = 0.50$), we neglect the κ_m contribution in the present analyses. A similarly very small κ_m was given also by Cohn et al. [16] for the $La_{1-X}Ca_XMnO_3$ system.

By using the Wiedemann–Franz (WF) law ($\kappa_e = L_0 T/\rho$; $L_0 = 2.45 \times 10^{-8}\,W\Omega/T^2$: the Lorentz number), we can estimate the electronic component $\kappa_e(T)$ of these crystals using the electrical resistivities. The estimated $\kappa_e(T)$ can be seen as an upper limit of the electronic part in $\kappa(T)$ [24]. Fig. 7(a) shows the electronic thermal conductivity $\kappa_e(T)$ for the FZ-NSMO crystal. In the respective magnetic fields, κ_e increases with decreasing T ($< T_c$) and reaches a maximum at T_N and then suddenly decreases with decreasing temperature T ($< T_N$). The electronic component has a large proportion to the total κ (e.g., κ_e immediately above T_N (= 160 K) is $\sim 24\%$ of the total κ at 0 T) and increases with increasing magnetic field. Fig. 7(b) shows the temperature dependence of the phonon thermal conductivity $\kappa_{ph}(T)$ of the FZ-NSMO crystal for each magnetic

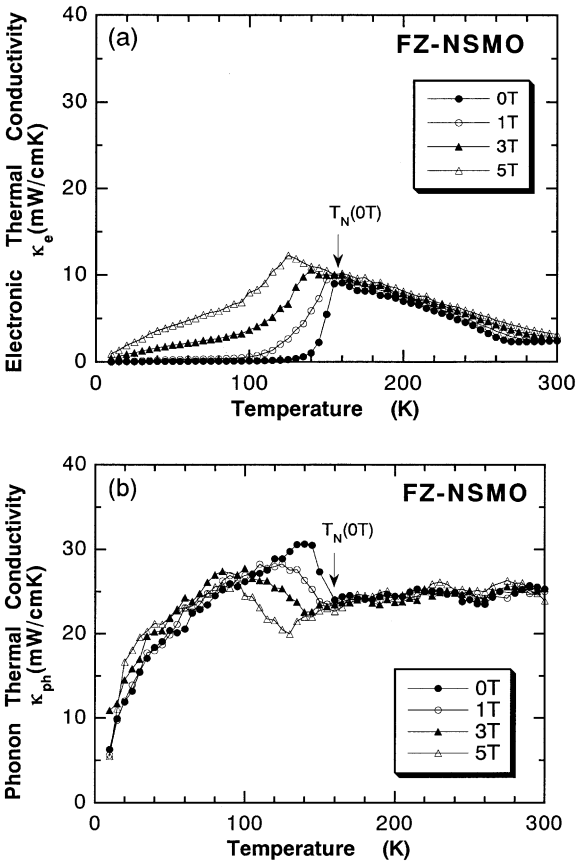

Fig. 7. Temperature dependence of (a) the electronic thermal conductivity $\kappa_e(T)$ and (b) the phonon thermal conductivity $\kappa_{ph}(T)$ of the FZ-NSMO crystal in applied fields. The Wiedemann–Franz law was applied for estimation of $\kappa_e(T)$.

field, which was estimated by subtracting the electronic contribution κ_e from the measured κ. What is to be noticed is that the phononic component κ_{ph} is sharply enhanced just below T_N, while it is nearly independent of the applied magnetic field in the temperature ranges above T_N (> 150 K) and at low temperature ($T < 100$ K). These results indicate that the observed magnetic field dependence of κ of FZ-NSMO can be interpreted as to come mainly from κ_e. The application of the WF law with the standard L_0 value is justifiable in FZ-NSMO because κ_{ph} hardly depends on the applied field. In general, $\kappa_{ph}(T)$ in condensed matter is determined by the strength of various phonon scattering mechanisms such as grain boundaries, various lattice defects, conduction electrons and so on [24]. In ordinary metals, the conduction electrons behave as main heat carriers and, at the same time, act as powerful scatterers to phonons. In this sense, the FZ-NSMO crystal is a pretty good metal in the ferromagnetic state between $T_N < T < T_c$, where the phonon scattering by conduction electrons is very effective. The phonon scattering by conduction electrons suddenly disappears in the charge ordered insulating phase below T_N, which is the main origin for the κ_{ph} enhancement below T_N.

Because of the large resistivity of the S-LSMO crystal, κ_e is very small. For example, the temperature dependence of $\kappa_e(T)$ is shown in Fig. 3. κ_e is about 5% of the total κ at 300 K and decreases with decreasing temperature. Therefore, the $\kappa(T)$ reductions below T_N of the measured $\kappa(T)$ shown in Fig. 3 mainly result from those of $\kappa_{ph}(T)$, which should originate from the enhancements in the phonon scattering related with the phase transition from FM to AF order.

There may be some problems about the applicability of the WF law to κ_e in polycrystals because of the difference in the electrical and thermal transport through the grain boundaries. It is conceivable that heat transport between grains can be easier than electric transport, thus making the effective Lorentz number much larger. Actually, several sintered LSMO samples showed anomalously large $\rho(T)$ values caused by inappropriate sintering or annealing processes. We carefully omitted such samples. In Fig. 3, $\kappa(T)$ of S-LSMO does not show any clear dependence on the applied field for $T > T_N(0T)$ and $T > T_N(5T)$. Because $\rho(T)$ of S-LSMO is larger in spite of a clear field dependence, this fact indirectly guarantees that κ_e is really small in S-LSMO.

As we have seen, the field dependence of the phonon thermal conductivities $\kappa_{ph}(T)$ of the FZ-NSMO and S-LSMO crystals shows quite different behavior below T_N. The field dependence of $\kappa(T)$ below T_N for the FZ-NSMO crystal shown in Fig. 6 is caused by the enhancement of κ_e as a result of the colossal magnetoresistance. The phonon scattering by conduction electrons, which is dominant at $T_N < T < T_c$, diminishes below T_N. It is possible that, actually, the reduction of the phonon scattering by conduction electrons screens the enhancement of the phonon scattering due to other mechanisms which appears at the first order magnetic transition in FZ-NSMO. It is also worthwhile to note that the phonon scattering by conduction electrons is almost absent in the FM semiconductive state of S-LSMO, making a marked contrast to FZ-NSMO.

5. Conclusion

The thermal conductivity $\kappa(T)$ has been measured for the sintered-$La_{0.50}Sr_{0.50}MnO_3$ (S-LSMO) and FZ-$Nd_{0.50}Sr_{0.50}MnO_3$ (FZ-NSMO) crystals in magnetic fields up to 5 T. The origin of the $\kappa(T)$ anomaly around the Néel temperature T_N was discussed. Important experimental results and the noticeable points obtained in this study are summarized as follows:

(1) In these crystals, $\kappa(T)$ shows seemingly similar reductions just below T_N in zero magnetic field. However, the field dependence of $\kappa(T)$ is quite different. $\kappa(T)$ of FZ-NSMO increases below T_N with increasing magnetic field, which can be interpreted as caused by the enhancement of the electronic thermal conductivity $\kappa_e(T)$. On the other hand, $\kappa(T)$ of the S-LSMO crystal does not depend on the magnetic field except for the shift of T_N because of the smaller κ_e. The reduction of $\kappa(T)$ below T_N in S-LSMO comes

from the reduction in the phonon component κ_{ph} caused by the phonon scattering enhancement.

(2) The phonon thermal conductivity $\kappa_{ph}(T)$ is enhanced below T_N in FZ-NSMO as shown in Fig. 7(b). The origin of the κ_{ph} enhancement is the elimination of the strong phonon scattering by the conductive charge carriers below T_N. It is plausible that $\kappa_{ph}(T)$ would be reduced also in FZ-NSMO, if it is not for the phonon scattering by the charge carriers in the FM metallic phase.

Acknowledgements

The author wishes to thank S. Sugawara and T. Mikami of Iwate University for their assistance in the sample preparation and in the thermal conductivity measurements. The author also wishes to thank Prof. K. Noto of Iwate University for the collaboration in using the cryocooled superconducting magnet. Useful discussion with Prof. M. Ikebe is greatly acknowledged.

References

[1] A.J. Millis, B.I. Shraiman, R. Mueller, Phys. Rev. Lett. 77 (1996) 175.
[2] P. Dai, Jiandi Zhang, H.A. Mook, S.-H. Liou, P.A. Dowben, E.W. Plummer, Phys. Rev. B 54 (1996) 3694.
[3] S.J.L. Billinge, R.G. Difrancesco, G.H. Kwei, J.J. Neumeier, J.D. Thompson, Phys. Rev. Lett. 77 (1996) 715.
[4] G. Zhao, Nature 381 (1996) 676.
[5] P. Schiffer, A.P. Ramirez, W. Bao, S.W. Cheong, Phys. Rev. Lett. 75 (1995) 3336.
[6] H. Kawano, R. Kajimoto, H. Yoshizawa, Y. Tomioka, H. Kuwahara, Y. Tokura, Phys. Rev. Lett. 78 (1997) 4253.
[7] H. Kuwahara, Y. Moritomo, Y. Tomioka, A. Asamitsu, M. Kasai, R. Kumai, Y. Tokura, Phys. Rev. B 56 (1997) 9386.
[8] H. Fujishiro, M. Ikebe, Y. Konno, J. Phys. Soc. Japan 67 (1998) 1799.
[9] R. Kajimoto, H. Yoshizawa, H. Kawano, H. Kuwahara, Y. Tokura, K. Ohoyama, M. Ohashi, Phys. Rev. B 60 (1999) 9506.
[10] C. Ritter, R. Mahendiran, M.R. Ibarra, L. Morellon, A. Maignan, B. Raveau, C.N.R. Rao, Phys. Rev. B 61 (2000) R9229.
[11] T. Akimoto, Y. Maruyama, Y. Moritomo, A. Nakamura, K. Hirota, K. Ohoyama, M. Ohashi, Phys. Rev. B57 (1998) 1.
[12] A. Moreo, S. Yunoki, E. Dagotto, Science 283 (1999) 2034.
[13] Y. Moritomo, private communication.
[14] P.G. Radaelli, M. Marezio, H.Y. Hwang, S.-W. Cheong, B. Batlogg, Phys. Rev. B 54 (1996) 8992.
[15] M.C. Martin, G. Shirane, Y. Endo, K. Hirota, Y. Moritomo, Y. Tokura, Phys. Rev. B 53 (1996) 14285.
[16] J.L. Cohn, J.J. Neumeier, C.P. Popoviciu, K.J. McClellan, Th. Leventouri, Phys. Rev. B 56 (1997) R8495.
[17] D.W. Visser, A.P. Ramirez, M.A. Subramanian, Phys. Rev. Lett. 78 (1997) 3947.
[18] J. Hejtmanek, Z. Jirak, Z. Armold, M. Marysko, S. Krupicka, C. Martin, F. Damay, J. Appl. Phys. 83 (1998) 7204.
[19] H. Fujishiro, M. Ikebe, in: H. Oyanagi, A. Bianconi (Eds.), Physics in Local Lattice Distortions, AIP, New York, 2001, p. 433.
[20] M. Ikebe, H. Fujishiro, T. Naito, K. Noto, J. Phys. Soc. Japan 63 (1994) 3107.
[21] Y. Konishi, Z. Fang, M. Izumi, T. Manako, M. Kasai, H. Kuwahara, M. Kawasaki, K. Terakura, Y. Tokura, J. Phys. Soc. Japan 68 (1999) 3790.
[22] H. Kuwahara, T. Okuda, Y. Tomioka, A. Asamitsu, Y. Tokura, Phys. Rev. Lett. 82 (1999) 4316.
[23] M. Ikebe, H. Fujishiro, S. Sugawara, Physica B 281&282 (2000) 496.
[24] R. Berman, Thermal Conduction in Solids, Clarendon Press, Oxford, New York, 1976.